

An FTIR Study of the Complex Melting Behavior of α -Lactalbumin[†]Hui Zhong,[‡] Rudolf Gilmanshin,[§] and Robert Callender^{*,§,||}*Department of Physics, City College of the City University of New York, New York, New York 10031, and
Department of Biochemistry, Albert Einstein College of Medicine, Bronx, New York 10461**Received: November 23, 1998*

We have studied the thermal denaturation of holo α -lactalbumin (α -LA) using FTIR spectroscopy by monitoring the absorbance of protein bands in the secondary structure sensitive amide I region. In agreement with results obtained by other techniques, a major cooperative melting transition is observed between 60 and 80 °C. This main transition is found to involve predominantly the unfolding of helical structures. Addition of excess Ca^{2+} ions raises the T_m of the cooperative melting transition but does not change the protein substructures involved in the transition. In addition to the main transition, there are at least two other distinct melting processes. One of them is gradual, is independent of excess Ca^{2+} , and occurs throughout the measured temperature range below the major cooperative transition. This melting process involves denaturation of α -LA's β -hairpin. The other melting process is affected by the addition of excess Ca^{2+} and involves the denaturation of helical structures. In the absence of excess calcium, this transition, occurring between 45 and 60 °C, strongly overlaps with the major cooperative melting. Our results indicate that the β -hairpin of α -LA is not directly stabilized by the bound calcium ion present in the holo protein and melts independently from the rest of the protein.

Introduction

α -Lactalbumin (α -LA) is a small globular protein containing 123 residues that consists of two domains connected by a small bridge section.^{1,2} The α -domain is made up of only helical structures (both α - and 3_{10} -helices). The β -domain includes a double-stranded β -hairpin and some helical structure.^{3,4} The structure of α -LA is stabilized by four disulfide cross-links. Two of them are in the α -domain, one is in the β -domain, and one is a part of the interdomain bridge. A distinctive feature of the β -domain is a Ca^{2+} binding site, which plays an important structural role.^{5,6} In absence of intrinsic bound Ca^{2+} ion (the apo protein), the protein is destabilized and melts at a much lower temperature (the temperature decrease is 20–40 °C, depending upon salt and its concentration) than holo α -LA.^{5,7} Holo α -LA can exist in three forms in equilibrium: in native, in unfolded, and in destabilized forms whose properties are somewhat intermediate with respect to the other two (see refs 8 and 9 for references). Specific destabilized forms have often been named molten globules. The balance of these three forms depends on conditions: buffer salt and its concentration, abundance of calcium, pH, temperature, and denaturant concentration. The molten globule is believed to resemble an intermediate on the protein folding pathway.^{8–12}

Because of these features, α -LA has been widely researched with regard to protein structure and thermodynamics and in protein folding studies.^{8,9} While in earlier denaturation work holo α -LA was treated as a whole, recent research on protein

with partially reduced disulfides and its mutants lacking some of the disulfides has shown that the α - and β -domains can fold independently under some conditions.^{3,4} The domains behave differently even on the level of a molten globule. Thus, in the acid destabilized form of α -LA, the α -domain remains in a nativelike topology while the β -domain is largely unstructured.¹³ However, under native conditions, the behavior of unmodified protein appears to undergo a highly cooperative denaturation process, as shown by equilibrium^{7,14} and kinetic¹⁵ folding studies. To investigate the controversy between the structural independence of domains and cooperative behavior of the protein molecule as a whole, folding studies are needed, probing selectively the substructures of the protein. When such a study was carried out by means of NMR for apo α -LA, the results suggested that the β -hairpin appears earlier than the rest of the protein structure.¹⁶

A number of studies have investigated the thermal unfolding/folding of holo α -LA.^{5,7,17–20} As judged by calorimetry, CD, and NMR spectroscopy, holo α -LA undergoes a cooperative transition with a T_m of around 65 °C. The presence of excess Ca^{2+} stabilizes the holo protein and shifts the transition 10 °C to higher temperatures.^{5,20} The detailed study of the temperature-denatured state had proved that it is compact, rich with secondary structure, and similar to the other intermediate states of holo α -LA.^{17,21} The extensive study of temperature-induced denaturation of holo α -LA has shown a complexity of melting, which includes several transitions.^{19,20} Previous interpretation of this complex melting has assumed a coexistence of the three forms of holo α -LA in the transition region: holo-native, holo-melted, and apo-melted forms.²⁰ However, there is very limited information on the specific structural nature of the various forms.

In this paper, we report a thermal denaturation study of intact α -lactalbumin by FTIR spectroscopy. Vibrational spectroscopy can monitor separately substructures within the intact protein and also be sensitive to fast interchanging forms. It has been

[†] This work was supported by grants from the National Science Foundation (MCB-9727439) and the Institute of General Medicine, National Institutes of Health (GM35183).

* Corresponding author: 718-430-3024 (voice); 718-430-8565 (fax); call@aeom.yu.edu (e-mail).

[‡] City College of the City University of New York New York.

[§] Albert Einstein College of Medicine.

^{||} On leave from City College of New York.

shown that helices, β -structure, and disordered backbone could be determined separately from the IR absorbance spectrum of α -LA in the amide I region.²² Therefore, IR spectroscopy can report the separate melting behavior of these elements of secondary structure. In agreement with previous studies, it is found that holo α -LA undergoes a major cooperative transition between 60 and 80 °C with T_m depending on calcium concentration. Besides this main transition, however, there are at least two other melting processes. One of them is a gradual process, independent of excess Ca^{2+} , which occurs throughout the low temperatures prior to the major cooperative melting and includes mostly the denaturation of the β -hairpin structure. Hence, our results indicate that the sole β -hairpin of holo α -LA melts independently from the rest of the protein. The second minor melting process depends on the concentration of extrinsic calcium and involves the helical structures of holo α -LA. When no excess calcium is added, the process strongly overlaps with the major cooperative melting. A previous FTIR thermal melting study of α -LA has been performed;²³ however, the protein aggregated at high temperatures. The results presented here are free of aggregation products even at the highest temperatures, presumably because of the lower concentrations used in our study.

Materials and Methods

Bovine α -lactalbumin (type I) was purchased from Sigma (St. Louis, MO) and was further purified with gel filtration on Sephadex G-75 in 0.1 M Tris buffer, pH 8.1 at 5 °C. Then, it was dialyzed against deionized water, lyophilized, and stored at -80 °C. The sample thus obtained was homogeneous on polyacrylamide gel electrophoresis in the presence of SDS. This procedure does not remove the calcium ion that is normally bound to the Sigma protein. Hence, all measurements reported herein are on the holo protein. Protein concentration was determined by optical absorbance at 280 nm using an extinction coefficient¹⁷ of $E_{1\%}^{1\text{cm}} = 20.9 \text{ cm}^{-1}$. α -LA concentrations of 8–10 mg/mL were used for IR measurements. The reported pH* values are uncorrected pH-meter readings at room temperature. All other chemicals were purchased from Sigma and were of the highest available purity.

The sample solutions were made in D_2O with 4 mM sodium cacodylate buffer (pH* 6.8) containing 10 mM KCl. pH* was adjusted by DCl and NaOD. To facilitate H–D exchange, the protein sample was incubated in D_2O at 55 °C for 2 h. Prior to the IR measurements, the protein solutions were equilibrated with the reference solvent on a Sephadex G-25 column. Both protein and buffer samples were collected from the same elution to ensure balanced HDO in both the reference and protein solutions. The sample aliquots after the column equilibration were used to control its pH* and concentration.

At the high concentrations required for the IR study, it is important to ensure that the observed transitions are both reversible and that the samples are free from aggregation products. Reversibility was verified by determining the melting curve as a function of increasing temperature, holding a high temperature for a fixed period and then performing a rescan of the melting curve toward lower temperatures. Only data from runs verified to be reversible are presented herein. IR absorption in the amide I' (the prime denotes deuterated peptide linkage) is quite sensitive to the formation of aggregates with marker bands at 1623 (strong) and 1680 (weak) cm^{-1} typical of an intermolecular β -structure showing up. It was found that prolonged exposure of the holo α -LA to a high temperature (above 80 and 70 °C in the absence and the presence of 10

mM CaCl_2 , respectively) resulted in irreversible denaturation (see also ref 5). The appearance of the irreversible fraction correlated with the characteristic bands at 1623 (strong) and 1680 (weak) cm^{-1} . Only the spectra free of the aggregation features were used for the analysis.

IR absorbance spectra were measured by an IFS-66 Fourier transform spectrometer (Bruker Instruments, Inc., Billerica, MA) using an MCT detector. Both reference and sample solutions were simultaneously loaded into a thermostated dual cell shuttle accessory. CaF_2 sandwich cells with 56 μm Teflon spacers were used. To prevent sample leakage at high temperature, thin smears of inert silicon grease on the spacer were used. No influence of the grease on data was found, at least below 65 °C where control measurements in the absence of the grease were possible. A two-position sample shuttle was used to alternate between the sample and buffer positions; this procedure substantially decreases the spectral contribution of residual water vapor after subtraction. A total of 26 repetitions of 32 scans were averaged for each of the two cells. Spectra were collected with 2 cm^{-1} resolution, and a Blackman-Harris three-term apodization was applied. Temperature, determined by a BAT-12 thermometer with a type IT-18 thermocouple microprobe attached directly to the cell surface (Physitemp Instruments, Inc., Clifton, NJ), was controlled with a Model 1167 bath circulator (VWR Scientific, S. Plainfield, NJ).

OPUS 2.0 (Bruker Instruments, Inc.) and Grams/386 (Galactic Industries Corp., Salem, NH) software were used for data collection and analysis. The solvent background spectrum was subtracted from each protein solution spectrum. As the sample and reference cells were assembled separately, their path lengths were not completely equal (the difference was within 5%). To correct for this, the solvent spectrum was multiplied by a correction factor determined by requiring a baseline flat between 1750 and 2000 cm^{-1} and by an accurate subtraction of D_2O absorption bands at 3840 cm^{-1} from solution and reference spectra.²⁴ No correction was introduced in solvent subtraction for the spectra intended for deconvolution and derivation to keep the residual water vapor background minimal.

The positions of band components in the amide I' region were determined by using both the second derivatives and deconvolved spectra. The second derivative spectra were calculated using the Savitzky–Golay algorithm (with a fourth-order polynome on a 19 data point window, which corresponds approximately to $\text{fwhh} = 20 \text{ cm}^{-1}$ for our data sets). Deconvolution, based on the method of Griffiths and Pariente,²⁵ was performed between 1530 and 1730 cm^{-1} with $\text{fwhh} = 25 \text{ cm}^{-1}$. A linear baseline was subtracted prior to deconvolution to ensure zero absorption at the ends of the spectral interval.

Results

Infrared absorbance spectra of holo α -LA at several temperatures are presented in Figure 1a. The region between 1610 and 1700 cm^{-1} contains mainly contributions of the amide I' band. It is formed by a complex vibrational mode that is dominated by the peptide group $\text{C}=\text{O}$ stretch (about 80%) with a minor contribution from the $\text{C}-\text{N}$ stretching vibration. This band is sensitive to the protein secondary structure.^{26,27} The absorbance between 1540 and 1620 cm^{-1} is due to side chain vibrations of aromatic groups as well as the asymmetric stretching mode of COO^- groups.²⁶ The amide II vibrations of some unexchanged peptide groups can also contribute to this region. The intrinsic bandwidths of the amide I' band components are often greater than a separation between neighboring bands. In this case, resolution enhancement techniques, such as derivation and

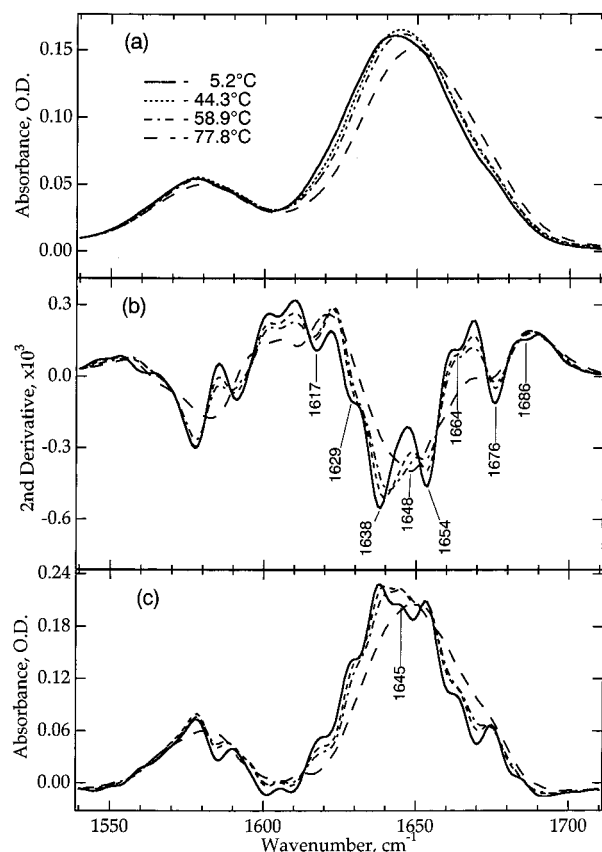


Figure 1. α -Lactalbumin IR absorbance spectra (a), their second derivatives (b), and deconvoluted spectra (c) at different temperatures. The protein concentration was 8.0 mg/mL. The spectra are presented at the temperatures corresponding to the borders of the intervals with different melting behavior (see text and Figure 3c).

deconvolution, have been shown to be useful in making assignments.²⁸ The second derivatives and deconvoluted spectra are presented in Figure 1b,c, respectively, and components at 1617, 1629, 1638, 1645, 1654, 1664, 1676, and 1686 cm^{-1} are clearly observed.

The measured spectra of native holo α -LA below 45 $^{\circ}\text{C}$ are similar to those in earlier studies^{22,29} except for differences between 1645 and 1668 cm^{-1} . Although the samples of the previous studies contained excess calcium ions, this is not the source of the discrepancy because the IR absorbance spectra of native holo α -LA contain the same components (although with different relative intensities) in the absence of extrinsic Ca^{2+} and in the presence of 10 mM of CaCl_2 (compare the low-temperature spectra in Figures 1 and 2). We believe that the small differences between the current study and previous results are due to incomplete deuterium exchange in the previous work. This is consistent with the observation of time dependent IR changes in those studies.^{22,29} In our case, deuterio exchange at an elevated temperature was performed before the addition of excess Ca^{2+} to the protein solution. However, in refs 22 and 29 the lyophilized protein was directly dissolved in the Ca^{2+} -containing buffer, which stabilizes the protein and decelerates an H-D exchange.

According to previous assignments between band position and secondary structure,^{22,29} the bands at 1638 and 1654 cm^{-1} correspond to 3_{10} - and α -helices, respectively, the 1629 and 1675 cm^{-1} bands to the low- and high-frequency components of the β -sheet structure, the 1668, 1675, and 1686 cm^{-1} peaks to unfolded structures, and the component at 1645 cm^{-1} to the

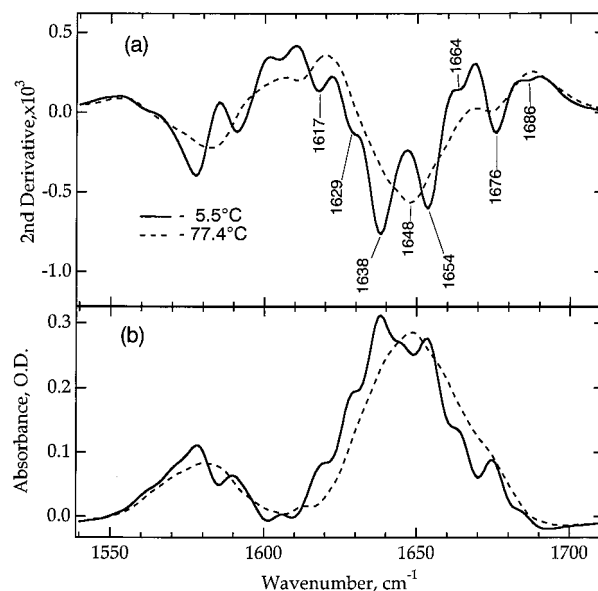


Figure 2. Second derivative (a) and deconvoluted spectra (b) in the amide I' region of α -lactalbumin in the presence of 10 mM of CaCl_2 at 5.5 and at 77.4 $^{\circ}\text{C}$. The protein concentration was 9.5 mg/mL.

disordered part of the polypeptide backbone. It is also possible that part of the intensity of the 1638 cm^{-1} band is due to an α -helical structure exposed to solvent, since it is known that a band at 1635–1645 cm^{-1} is observed for model polypeptide α -helices and in destabilized α -helical proteins (see refs 30–34 and references therein). However, the spectrum of these so-called “solvated” helices is generally characterized by a rather wide band, and they exhibit very gradual melting dependence with low cooperativity.^{32,34–36} In the case of holo α -LA, neither second derivative nor deconvoluted spectra show any difference between the widths of 1638 and 1654 cm^{-1} bands, and moreover, the major change in cooperative melting (see below) is found to come from the 1638 cm^{-1} component. Therefore, most, if not all, of the intensity from the 1638 cm^{-1} component arises from the 3_{10} -helix in α -LA.

The amide I' band of the α -LA at 78 $^{\circ}\text{C}$ (Figure 1) is essentially featureless, even after deconvolution, and is dominated by a wide band centered near 1648 cm^{-1} . Only a small band near 1674 cm^{-1} is otherwise evident in the second derivative and deconvoluted spectra. Similar wide spectra with maxima at 1642–1650 cm^{-1} and shoulders at higher frequencies were found for several proteins that have been temperature denatured (see ref 37 and references therein) and disordered polypeptides.^{32,38} Such a spectrum does not mean that the temperature-denatured protein is structureless, because fluctuating elements of the secondary structure may result in wide components that cannot be detected with derivation or deconvolution. For example, considerable helicity and a small but tightly packed “core” of residues was detected by means of enhanced equilibrium and kinetics studies of the acid apoMb-E form of apomyoglobin, and this form has an IR absorbance spectrum very similar to the high-temperature spectrum of holo α -LA (R. Gilmanshin, R. H. Callender, R. B. Dyer, manuscript in preparation). Therefore, although the comparison of the spectra measured at different temperatures (Figure 1) shows that the decrease of intensity of the secondary structure components is accompanied by a concomitant intensity increase of the disordered structure bands, we believe it cannot be concluded that there is no secondary structure in the melted form of holo α -LA as previously suggested.^{17,21}

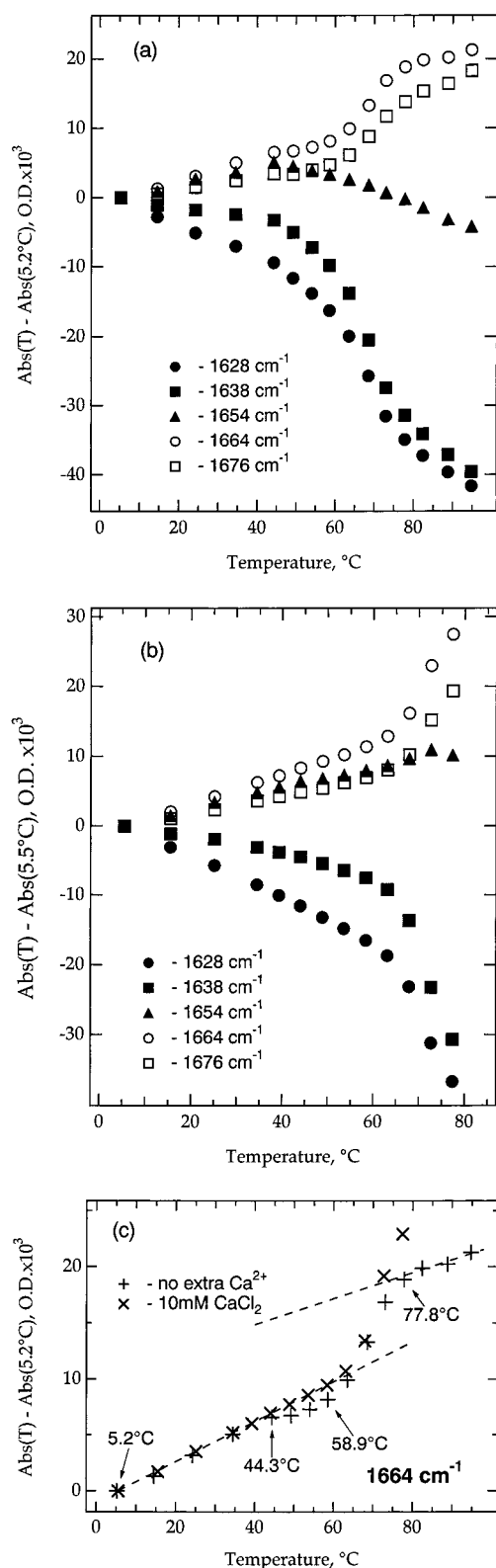


Figure 3. Temperature dependences of α -lactalbumin IR absorbance at 1628, 1638, 1654, 1664, and 1676 cm^{-1} , without extra calcium (a) and in the presence of 10 mM CaCl_2 (b). The dependences measured at 1664 cm^{-1} are superimposed for clarification in panel c. The data measured with 10 mM CaCl_2 are divided by 1.2 to compensate for the concentration difference. The dashed lines show the linear baselines of the melting transition without extra calcium. The arrows show temperatures at which the spectra presented at Figure 1 were measured.

The temperature dependencies of IR absorbance at different wavenumbers for holo α -LA are presented in the Figure 3

without (3a) and with (3b) excess calcium. The wavenumbers corresponding to the minima of the second derivative were chosen because the changes in composition of the corresponding secondary structure components are dominant at these frequencies. The major sigmoidal transition of holo α -LA in Figure 3a is obvious between 60 and 80 $^\circ\text{C}$ with a T_m near 66–69 $^\circ\text{C}$. A more accurate determination of the T_m is complicated by nonlinear changes starting before but overlapping the sigmoidal transition. A similar but slightly lower value of the T_m (62–67 $^\circ\text{C}$) has been reported previously.^{5,7,17,20} The apparent increase of the melting temperature is not due to some excess calcium that is present in the solution because of solubility of the IR cell CaF_2 windows, since the solubility of CaF_2 is very low (<0.2 mM). The difference in T_m is almost certainly from a stabilization of the native form in the presence of the D_2O environment.^{39,40}

Three melting regions can be identified from the data of Figure 3: a linear melting region (from 5 to 45 $^\circ\text{C}$); a nonlinear melting region or pretransition region (from 45 to 60 $^\circ\text{C}$); and the major sigmoidal transition region (60–80 $^\circ\text{C}$). The addition of excess CaCl_2 (10 mM) produces two obvious effects on the melting behavior of holo α -LA (Figure 3b,c). First, the T_m is shifted to a higher temperature, ≥ 70 $^\circ\text{C}$, as previously observed.^{5,20} The second effect is the disappearance of the changes that take place in the pretransitional melting region. The baseline is linear through the whole temperature range below the sigmoidal melting transition. The IR absorbance spectra at the temperatures separating the melting regions are presented in Figure 1a.

The observed changes in IR absorbance originate from some protein structure transformation rather than from nonspecific temperature dependence of spectral parameters. The nonspecific temperature dependence of IR bands in this spectral region, which are known to be small, have not been systematically studied. This is because it is difficult to separate the effects of structural changes from nonspecific temperature changes. In general, changes in the slope of intensity versus temperature are taken as indicative of structural changes. The three regions are especially obvious in the melting curve measured at 1654 and 1664 cm^{-1} (Figure 3a; see also Figure 3c), where the pretransition region exhibits a change in sign opposite to both the linear melting and sigmoidal denaturation transition changes. At 1654 cm^{-1} , which is close to the isosbestic point of the main denaturation transition, the pretransition effect shows up as a slope change of the dependence at 45 $^\circ\text{C}$. Also, it is clear from Figure 3c that excess calcium changes the temperature response of the IR intensity, an effect not expected for a nonspecific temperature dependence. Moreover, measurements performed on isolated peptides over a 70 $^\circ\text{C}$ temperature range show that the temperature dependence of IR bands in this region is less than 0.2% in intensity change relative to the maximum absorbance over any 10 $^\circ\text{C}$ (R. B. Dyer, private communication). Our studies³⁵ of apomyoglobin, over approximately the same range where the pretransitional change in α -LA occurs, show less than a 1% change in intensity using the marker band associated with buried helix (i.e., a structure that does not melt until a higher temperature). Experiments⁴¹ on RNase A, a very stable protein, show less than a 2% absolute change at any wavelength below the major melting transition, and the data show a very crisp isosbestic point with less than a 0.6% change over the entire 20–80 $^\circ\text{C}$ temperature range, which encompasses the major melting transition. Hence, the nonspecific temperature dependence of the IR bands is less than 0.6% and is probably less than 0.2%. The changes in Figure 3 are greater than 1.5%,

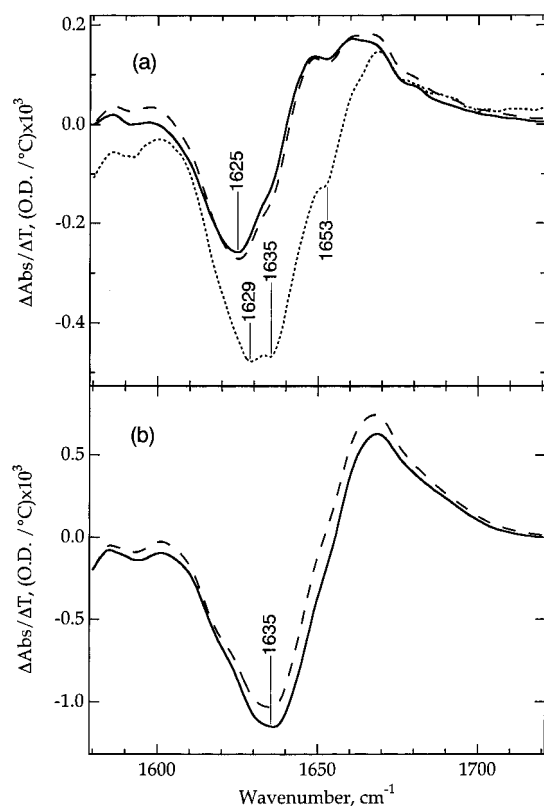


Figure 4. Difference spectra of α -lactalbumin in the amide I' region reduced to per degree centigrade for different temperature intervals: prior (a) and within (b) the major melting transition. Panel a: linear melting regime without extra calcium (bold line, calculated for the 44.3–5.2 °C interval) and in the presence of 10 mM CaCl_2 (dashed line, 58.4–5.5 °C); pretransition nonlinear melting without extra calcium (dotted line, 58.9–44.3 °C). Panel b: major melting transition without extra calcium (bold line, 77.8–58.9 °C) and in the presence of 10 mM CaCl_2 (dashed line, 77.4–58.4 °C). The spectrum at the lower temperature was subtracted from a higher temperature spectrum. The spectra with excess Ca^{2+} are divided by 1.2 to compensate for the concentration difference.

as determined by the reversal in slope that occurs in the 1654 cm^{-1} band before the main melting transition (Figure 3a).

Figure 4 plots the spectral difference between the high-temperature point and the low-temperature point, divided by the temperature change to reduce the presented effect to changes per degree centigrade, for the linear and the nonlinear pretransition regions (Figure 4a), and the sigmoidal region (Figure 4b). The results from runs with and without excess Ca^{2+} ions are shown. This method of presentation elucidates the details of the spectral changes with temperature.

The linear region is characterized by several sharp negative bands in the difference spectrum of panel 4a. The most intense band is at 1625 cm^{-1} , corresponding to the band found at 1629 cm^{-1} in the low-temperature α -LA spectrum. Other weaker bands are located at 1635, 1653, and 1676 cm^{-1} (corresponding to the 1638, 1654, and 1676 cm^{-1} bands). The intensities of these bands decrease with increasing temperature, and their intensities are traded for the wider disordered bands at 1648 and 1673 cm^{-1} , characteristic of disordered structure. The apparent displacements of the difference spectrum bands from their positions found in the amide I' absorbance spectra (see Figures 1 and 2) are most probably due to the fact that in the difference spectrum they overlap with the steep wings of the disordered structure band of opposite sign. According to previous assignments, the observed changes in the difference

spectrum show that substantial melting of the β -structure occurs with a smaller decrease of helical content. The spectral changes within the linear region are quantitatively the same in the presence and absence of additional extrinsic calcium. Hence, it can be concluded that additional Ca^{2+} (apart from the Ca^{2+} ion of the holo protein) does not stabilize the substructure which is melted at low temperatures.

In the pretransition region (dotted line, Figure 4a), both the β -structure (band at 1629 cm^{-1}) and substantially larger amounts of helices (see minima at 1635 and 1653 cm^{-1} on the difference spectrum) are melted. These helices are contained in a substructure that is stabilized by additional protein-bound Ca^{2+} ion(s) because the addition of 10 mM CaCl_2 shifts this pretransitional melting to higher temperatures and the spectral changes are the same throughout all the temperatures below the major cooperative melting (compare the spectral differences corresponding to the linear regions in Figure 4a).

In the cooperative melting temperature region (sigmoidal transition, Figure 4b), the major change in the difference spectrum is the loss of signal at 1635 cm^{-1} . Hence, the major structure elements disrupted within the cooperative transition are 3_{10} -helices and/or solvated α -helices. Small negative shoulders can also be found at 1629, 1654, and 1676 cm^{-1} , indicating some melting of β -sheet, native α -helix, and turns. These small changes may be due to overlapping of the cooperative transition with the linear melting process, at least partially. It is possible that substantially more of the native helix melts in the cooperative transition than is shown by the IR results. The marker position of native α -helix at 1654 cm^{-1} is close to the position of the maximum (ca. 1648 cm^{-1}) of the absorbance spectrum of the melted protein (Figure 1). Therefore, it is possible that a decrease at 1654 cm^{-1} with temperature is matched by an increase of a disordered structure absorbance. The denaturation spectral effects within the cooperative melting transition are the same in both the presence and absence of excess calcium. Hence, the addition of excess CaCl_2 only shifts the transition temperature but does not change the protein substructures involved in the transition.

Unfortunately, the thermodynamic parameters of the melting cannot be determined accurately from the IR data. In the presence of additional CaCl_2 , a progressive aggregation begins at high temperatures before the end of the transition which hinders an accurate determination of the high-temperature baseline. If no extra Ca^{2+} is added, the nonlinear pretransition process overlaps with the sigmoidal transition, and this results in nonlinear van't Hoff plots. However, for the sigmoidal transition as monitored at 1627 cm^{-1} (the effects of the nonlinear transitions here are minimal because the participating bands are at higher wavenumbers), an estimation of 230 kJ/mol could be obtained for the transition enthalpy. This is smaller than the values of 250⁴² or 295 kJ/mol¹⁷ obtained by scanning calorimetry in similar conditions in H_2O . However, a small decrease of melting enthalpy is expected for the melting in D_2O .³⁹

Discussion

Our results indicate that holo α -LA melting includes at least three different processes. One, a cooperative melting transition with a T_m at 62–67 °C, has been observed in previous studies.^{5,7,17,20} In agreement with these studies, the T_m of this transition is raised by the addition of excess calcium and involves mostly the melting of helices. An accurate estimation of how much helical structure melts is not possible due to the strong overlapping of their negative going bands upon melting with the positive going bands from the denatured polypeptide chain (see also Results).

In addition, between 5 and 45 °C, a gradual melting of the holo protein in a Ca^{2+} independent process is also observed. Its quasi-linear temperature dependence shows low (if any) cooperativity in this melting process.¹⁴ According to our data, in combination with the published assignments of amide I' bands to secondary structure, the observed spectral changes are attributed to the loss of β -structure. This noncooperative melting process has been reported previously from the results of other techniques (see ref 14 and references therein), and it was proposed that this transition represents some unfolding of the α -domain.¹⁴ However, our results show that the gradual melting involves mostly β -structure and, hence, the β -domain, which contains the only β -structure (the β -hairpin) of holo α -LA.

It is not simple to estimate what proportion of the β -structure melts gradually prior the major transition because its amide I' band (1629 cm^{-1}) overlaps strongly with the side chain (1618 cm^{-1}), helical (1638 cm^{-1}), and disordered structure (1648 cm^{-1}) bands. As an estimate, we take the absorbance at 1625 cm^{-1} to be a measure of the amount of β -structure because this is the frequency of the maximal effect in the linear temperature region (cf. Figure 4a) and because the overlap of the helical and disordered structure bands is comparatively small. Further, we assume that the β -hairpin (residues 40–50 of α -LA) is completely intact at 5.2 °C and is basically melted at 95.3 °C (the lowest and highest temperatures of our measurements). In this case, the total absorbance change between 5.2 and 94.7 °C is 41 Milli-OD at 1625 cm^{-1} . In the gradual melting region (from 5.5 to 63.1 °C using the longer range in the presence of 10 mM CaCl_2), the total change in intensity at 1625 cm^{-1} is 19 mOD. The former range includes the melting of β -sheet structure as well as other structure(s), whereas the latter has to do only with the melting of β -structure. Hence, at least 46% of the β -structure has melted noncooperatively. The actual proportion is almost certainly larger because of additional absorbance at 1625 cm^{-1} due to the overlapping of neighbor bands.

A third melting process is also observed that takes place at intermediate temperatures, 45–60 °C, just prior to the cooperative transition ("pretransitional process"). This process involves a substantial decrease of helical substructures (components at 1638 and 1654 cm^{-1}). Contrary to the β -structure loss from 5 to 45 °C, this process is sensitive to the presence of excess Ca^{2+} , like the cooperative melting process. Also like the cooperative melting process, the pretransitional melting involves the melting of helices.

In summary, the results suggest that the β -domain of holo α -LA contains two substructures that melt independently from each other. One melts gradually, i.e., noncooperatively, and involves the β -hairpin of the β -domain. Since the β -domain contains the structurally important Ca^{2+} binding site, it seems clear that the β -domain includes also another substructure, at least partially. The melting of the second substructure is involved in one or both of the other two transitions, because both of them are influenced by the presence of excess Ca^{2+} ions. That the two melting processes occur independently of each other and one process is dependent on excess calcium ions while the other is not is not unreasonable given the β -domain structure of α -LA. The β -hairpin of the β -domain does not include residues in direct contact with the Ca^{2+} ion;^{1,6} hence, it seems possible that the β -hairpin of the β -domain could melt independently from holo α -LA's Ca^{2+} -binding domain. The Ca^{2+} -binding site is formed by the 3_{10} -helix G in the β -domain (residues 76–82) and α -helix C (86–99), which is assigned to either the α -⁴ or β -domain³ by different authors. Hence, the structure of the protein also is

consistent with the melting of helices that is observed in the calcium dependent processes. Our results do not address directly whether helices of the α -domain melt in the two calcium dependent processes, but we believe that it is likely that they do given the sigmoidal nature of the cooperative melting process. In any case, an important result from this investigation is that the melting of α -LA occurs in substructures that are not in a one to one identity with its domains as defined by its crystallographic structure. Such heterogeneous melting behavior has also been found in apomyoglobin.^{35,36}

The complex melting behavior of α -LA has been studied previously using calorimetry and near-UV circular dichroism.²⁰ The proposed model explained the melting complexity due to the coexistence of two denatured forms: with (holo-denatured) and without (apo-denatured) a Ca^{2+} ion at the calcium binding site. The latter apo-denatured form was assumed more disordered than the former one. It was estimated that the change of free energy accompanying Ca^{2+} release from native structure was large; hence, such a step would more likely occur after formation of the holo-denatured form. The addition of extra CaCl_2 increases the relative proportion of the holo-denatured form at lower temperatures, which allowed the authors²⁰ to explain the apparent high-temperature shift of the denaturation transition. According to this model,²⁰ it is possible to speculate that the pretransitional calcium dependent melting at 45–60 °C found here is the result of the production of the holo-denatured form. The observed major transition results from the further transformation of the holo-denatured form into the apo-form. In this case, the presence of extra 10 mM CaCl_2 should increase the proportion of the holo-denatured form after the first transition, shifting the calcium ion release to a higher temperature. However, this implies that pretransitional melting would show up in the IR melting curves with or without the addition of excess calcium except for a change of amplitude (since calcium presumably affects the proportion of holo-denatured to apo-denatured forms). This is not observed since the first Ca^{2+} dependent melting transitions have different signs in the absence and presence of extra calcium (Figure 3c). Hence, the model of Vanderheeren and co-workers²⁰ does not fit our data very well, although it may apply to the major cooperative melting. In this case, another explanation for the pretransitional melting is necessary.

There are two possibilities. One is that the Ca^{2+} ion is released from native α -LA at a high temperature prior to the major cooperative melting. In this case, the pretransitional melting would involve an equilibrium between unmelted holo α -LA and apo-denatured α -LA since it is known that α -LA without Ca^{2+} melts at temperatures lower than what is observed in the pretransitional region. This model for thermal-denatured holo α -LA would imply that the main transition involves the melting of helices involved in calcium-binding. This would explain why the pretransition melting disappears in the presence of excess CaCl_2 . Our favored explanation, however, is that the pretransition calcium dependent melting at 45–60 °C results from a different process that involves a second Ca^{2+} -binding site. Indeed, previous studies^{5,43} of bovine α -LA have indicated a second low-affinity Ca^{2+} -binding site, and a recent crystallographic study on human lactalbumin reveals a second calcium binding site. In the human protein, the second binding site is located on the protein's surface and not connected to its β -sheet structure. We note that a second binding site, which undergoes calcium release before the major melting transition, can also explain the difference of the results obtained by Vanderheeren et al.²⁰ in an analysis of their CD and calorimetric data.

References and Notes

- (1) Acharya, K. R.; Stuart, D. I.; Walker, N. P. C.; Lewis, M.; Phillips, D. C. *J. Mol. Biol.* **1989**, *208*, 99–127.
- (2) Acharya, K. R.; Ren, J.; Stuart, D. I.; Phillips, D. C.; Fenna, R. E. *J. Mol. Biol.* **1991**, *221*, 571–581.
- (3) Hendrix, T. M.; Griko, Y.; Privalov, P. *Protein Sci.* **1996**, *5*, 923–931.
- (4) Wu, L. C.; Schulman, B. A.; Peng, Z. Y.; Kim, P. S. *Biochemistry* **1996**, *35*, 859–63.
- (5) Kuwajima, K.; Harushima, Y.; Sugai, S. *Int. J. Peptide Protein Res.* **1986**, *27*, 18–27.
- (6) Stuart, D. I.; Acharya, K. R.; Walker, N. P. C.; Smith, S. G.; Lewis, M.; Phillips, D. C. *Nature* **1986**, *324*, 84–87.
- (7) Griko, Y. V.; Freire, E.; Privalov, P. L. *Biochemistry* **1994**, *33*, 1889–1899.
- (8) Kuwajima, K. *Proteins: Structure, Function, Genetics* **1989**, *6*, 87–103.
- (9) Ptitsyn, O. B. In *Protein Folding*; Creighton, T., Ed.; W. H. Freeman and Co.: New York, 1992; pp 243–300.
- (10) Kim, P. S.; Baldwin, R. L. *Annu. Rev. Biochem.* **1990**, *29*, 631–660.
- (11) Christensen, H.; Pain, R. H. *Eur. Biophys. J.* **1991**, *19*, 221–229.
- (12) Arai, M.; Kuwajima, K. *Folding Design* **1996**, *1*, 275–87.
- (13) Wu, L. C.; Peng, Z. Y.; Kim, P. S. *Nature Struct. Biol.* **1995**, *2*, 281–286.
- (14) Privalov, P. L. *J. Mol. Biol.* **1996**, *258*, 707–25.
- (15) Balbach, J.; Forge, V.; Vannuland, N. A. J.; Winder, S. L.; Hore, P. J.; Dobson, C. M. *Nature Struct. Biol.* **1995**, *2*, 865–870.
- (16) Balbach, J.; Forge, V.; Lau, W. S.; Van Nuland, N. A. J.; Brew, K.; Dobson, C. M. *Science* **1996**, *274*, 1161–1163.
- (17) Dolgikh, D. A.; Abaturov, L. V.; Bolotina, I. A.; Brazhnikov, E. V.; Bychkova, V. E.; Bushuev, V. N.; Gilmanshin, R. I.; Lebedev, Y. O.; Semisotnov, G. V.; Tiktupulo, E. I.; Ptitsyn, O. B. *Eur. Biophys. J.* **1985**, *13*, 109–121.
- (18) Permyakov, E. A.; Morozova, L. A.; Burstein, E. A. *Biophys. Chem.* **1985**, *21*, 21–31.
- (19) Vanderheeren, G.; Hanssens, I. *J. Biol. Chem.* **1994**, *269*, 7090–7094.
- (20) Vanderheeren, G.; Hanssens, I.; Meijberg, W.; Van Aerschot, A. *Biochemistry* **1996**, *35*, 16753–16759.
- (21) Dolgikh, D. A.; Gilmanshin, R. I.; Brazhnikov, E. V.; Bychkova, V. E.; Semisotnov, G. V.; Venyaminov, S. Y.; Ptitsyn, O. B. *FEBS Lett.* **1981**, *136*, 311–315.
- (22) Prestrelski, S. J.; Byler, D. M.; Thompson, M. P. *Int. J. Peptide Protein Res.* **1991**, *37*, 508–512.
- (23) Stokkum, I. H. M.; Linsdell, H.; Hadden, J. M.; Haris, P. I.; Chapman, D.; Bloemendal, M. *Biochemistry* **1995**, *34*, 10508–10518.
- (24) Venyaminov, S. Y.; Braddock, W. D.; Prendergast, F. G. *Biophys. J.* **1996**, *70*, A65.
- (25) Griffiths, P. R.; Pariente, G. L. *Trends Anal. Chem.* **1986**, *5*, 209–215.
- (26) Susi, H.; Byler, D. M. *Methods Enzymol.* **1986**, *130*, 290–311.
- (27) Jackson, M.; Mantsch, H. H. *Crit. Rev. Biochem. Mol. Biol.* **1995**, *30*, 95–120.
- (28) Arrondo, J. L. R.; Muga, A.; Castresana, J.; Goni, F. M. *Prog. Biophys. Mol. Biol.* **1993**, *59*, 23–56.
- (29) Prestrelski, S. J.; Byler, D. M.; Thompson, M. P. *Biochemistry* **1991**, *30*, 8797–8804.
- (30) Chirgadze, Y. N.; Brazhnikov, E. V. *Biopolymers* **1974**, *13*, 1701–1712.
- (31) Haris, P. I.; Chapman, D. *Biopolymers* **1995**, *37*, 251–263.
- (32) Martinez, G.; Millhauser, G. *J. Struct. Biol.* **1995**, *114*, 23–27.
- (33) Reisdorf, W. C., Jr.; Krimm, S. *Biochemistry* **1996**, *35*, 1383–6.
- (34) Williams, S.; Causgrove, T. P.; Gilmanshin, R.; Fang, K. S.; Woodruff, W. H.; Callender, R. H.; Dyer, R. B. *Biochemistry* **1996**, *35*, 691–697.
- (35) Gilmanshin, R.; Williams, S.; Callender, R. H.; Woodruff, W. H.; Dyer, R. B. *Proc. Natl. Acad. Sci. U.S.A.* **1997**, *94*, 3709–3713.
- (36) Gilmanshin, R.; Williams, S.; Callender, R. H.; Woodruff, W. H.; Dyer, R. B. *Biochemistry* **1997**, *36*, 15006–15012.
- (37) Fabian, H.; Mantsch, H. H. *Biochemistry* **1995**, *34*, 13651–13655.
- (38) Chirgadze, Y. N.; Shestopalov, B. V.; Venyaminov, S. Y. *Biopolymers* **1973**, *12*, 1337–1351.
- (39) Makhatadze, G. I.; Clore, G. M.; Gronenborn, A. M. *Nature Struct. Biol.* **1995**, *2*, 852–855.
- (40) Parker, M. J.; Clarke, A. R. *Biochemistry* **1997**, *36*, 5786–5794.
- (41) Reinstadler, D.; Fabian, H.; Backmann, J.; Naumann, D. *Biochemistry* **1996**, *35*, 15822–15830.
- (42) Pfeil, W. *Biophys. Chem.* **1981**, *13*, 181–186.
- (43) Berliner, L.; Koga, K.; Nishikawa, H.; Scheffler, J. E. *Biochemistry* **1987**, *26*, 5769–5774.